



ACCEPTED MANUSCRIPT

This is an early electronic version of an as-received manuscript that has been accepted for publication in the Journal of the Serbian Chemical Society but has not yet been subjected to the editing process and publishing procedure applied by the JSCS Editorial Office.

Please cite this article as M. Mohamed, B. Hani, F. D. Koca, G. Unal, N. A. Rahman, A. Basma, N. M. Bozkurt, A. A. M. Bachir, and H. Daoud, *J. Serb. Chem. Soc.* (2025) <https://doi.org/10.2298/JSC240915008M>

This “raw” version of the manuscript is being provided to the authors and readers for their technical service. It must be stressed that the manuscript still has to be subjected to copyediting, typesetting, English grammar and syntax corrections, professional editing and authors’ review of the galley proof before it is published in its final form. Please note that during these publishing processes, many errors may emerge which could affect the final content of the manuscript and all legal disclaimers applied according to the policies of the Journal.



J. Serb. Chem. Soc. **00(0)** 1-20 (2025)
JSCS-13048

Evaluation of antimicrobial, anticancer, and neuroprotective activities of silver nanoparticles (AgNPs) green-synthesized using a red pigment produced by *Streptomyces* sp. A23 strain isolated from Algerian bee pollen

MOKHNACHE MOHAMED^{1*}, BELHADJ HANI¹, FATIH DOGAN KOCA², GOKHAN UNAL³, NASRAT ABDUL RAHMAN⁴, AYSEGUL BASMA², NUH MEHMET BOZKURT³, AHMED ALIEN MOHAMED BACHIR¹ AND HARZALLAH DAUD¹

¹Applied Microbiology Laboratory, Natural Sciences and Life Faculty, Ferhat Abbas Setif 1 University, Setif, 19137, Algeria, ²Aquatic Animals and Diseases Laboratory, Veterinary Medicine Faculty, Erciyes University, Talas, 38280, Kayseri, Turkey, ³Pharmacology Department, Pharmacy Faculty, Erciyes University, Talas, 38280, Kayseri, Turkey, and ⁴Institute of Natural and Applied Science, Erciyes University, Talas, 38280, Kayseri, Turkey.

(Received 15 September 2024; revised 8 October 2024; accepted 15 January 2025)

Abstract: In this work, the red pigment of *Streptomyces* sp. A23 strain isolated from Algerian bee pollen was used for the green synthesis of silver nanoparticles (AgNPs) as well as for evaluating their antimicrobial, anticancer, and neuroprotective activities. AgNPs were synthesized as a result of the reduction of 1 mM and 5 mM silver nitrate solutions at various pH values (5, 7 and 9), and were subsequently characterized. AgNPs (5 mM, pH 9) exhibited a maximum UV-vis absorbance at 433 nm. DLS revealed that the average diameter was 112 nm. A zeta potential peak was found at -33 mV corresponding to increased stability. XRD analysis confirmed the crystallization nature of the material. Furthermore, FT-IR analysis revealed specific functional groups at 3471 cm⁻¹ to 478 cm⁻¹. In addition, FE-SEM showed that the mean size of the spherical AgNPs was 54.5 nm in diameter. The presence of Ag was revealed by EDX analysis. Additionally, good antimicrobial activity was observed against *E. faecalis* ATCC 19433, *C. albicans* ATCC 10231, *S. aureus* ATCC 6538P, *P. aeruginosa* ATCC 27853, *B. subtilis* ATCC 6633, *K. pneumoniae* ATCC 13883 and *E. coli* ATCC 7839, with inhibition zones of 32, 30, 30, 27, 25, 20 and 19 mm, respectively. The lowest MIC and MBC were recorded against *B. subtilis* ATCC 6633 with a value of 62.5 µg mL⁻¹. Intriguingly, all the synthesized AgNPs at concentrations of 2, 4, and 8 µg mL⁻¹ had cytotoxic effects on SH-SY5Y neuroblastoma cell lines. In addition, AgNPs (1 mM, pH 7) exhibited significant neuroprotective activity at the lowest tested concentration. Finally, AgNPs

* Corresponding author. E-mail: mmokhnache@yahoo.fr
<https://doi.org/10.2298/JSC240915008M>

synthesized using the red pigment of *Streptomyces* sp. strain A23 are promising therapeutic agents.

Keywords: actinomycetes; microbial pigment; green synthesis; antimicrobial activity; cancer; neuroprotective activity.

INTRODUCTION

Recently, the utilisation of nanomaterials in the medical field has attracted increased amounts of attention, especially as novel and alternative therapeutic agents with multifaceted applications.¹ One of these nanomaterials is silver nanoparticles (AgNPs), which are emerging as possible hopeful alternatives due to their beneficial features.² Two conventional methods were applied to synthesize AgNPs; chemical and physical methods. Due to their undesirable disadvantages, suitable and green alternative methods must be found. Among these methods, the biological methods which use bacteria, fungi, algae, plants, and others; have gained substantial prominence due to their high safety.³ Many researchers have used Actinomycetes, including *Streptomyces* bacteria to synthesize AgNPs.^{4,5} The genus *Streptomyces* is known as a source of valuable and variety of secondary metabolites, which are excellent tools for the green synthesis of nanoparticles.^{6,7} One such secondary metabolite is pigments which not only serve as an identifier product for *Streptomyces*, but also demonstrate a prominent potential for synthesizing AgNPs.⁸ This process of synthesis provides a fast, safe, and eco-friendly approach, and imparts significant biological properties like antioxidant, antimicrobial, and antiproliferative activities, to the resulting nanoparticles, which hold promise as multifaceted therapeutic agents capable of treating both communicable and noncommunicable diseases.^{9,10} Regarding communicable diseases, the growth of antibiotic-resistant microorganisms is one of the most important public health problems, which have emerged as a global crisis, underscoring the urgent need to discover novel and alternative antimicrobial agents to the conventional antibiotics.¹¹ AgNPs synthesized using secondary metabolites produced by *Streptomyces* exhibit good antimicrobial effects against a wide range of pathogenic microorganisms, including bacteria and fungi.¹² Moreover, when AgNPs are combined with conventional antibiotics, they can have synergistic effects that may overcome antibiotic resistance.¹³ For noncommunicable diseases, cancer and neurodegenerative disorders remain major health concerns, necessitating the discovery of new effective therapeutic agents.^{14,15} AgNPs synthesized using the microbial pigments have shown promising anticancer and neuroprotective effects.^{12,16} These nanoparticles are promising agents in cancer therapy because they can target the cancer cells, while avoiding the cells that are normal.¹⁷ Furthermore, the distinctive physicochemical properties of these nanoparticles allow them to exhibit antioxidant activities, reducing the oxidative stress that might lead to neurodegenerative disorders. Additionally, these

nanoparticles can modulate inflammatory responses, further contributing to their neuroprotective effect.¹⁸

Therefore, this study aims to synthesize AgNPs using a red pigment produced by the *Streptomyces* sp. A23 strain isolated from Algerian bee pollen as a new biological reducing agent to evaluate their antimicrobial, anticancer, and neuroprotective activities.

EXPERIMENTAL

Materials

Silver nitrate (AgNO₃), hydrogen peroxide (H₂O₂), and dimethyl sulfoxide (DMSO) were purchased from Sigma. Muller-Hinton broth was obtained from Conda, and carbonate calcium (CaCO₃) was obtained from Merck. The GF-1 Nucleic Acid Extraction Kit, universal primers (27F and 1492R), and Clean-Up Kit were from Vivantis Technologies. Gentamicin discs were provided from Oxoid™. *Staphylococcus aureus* ATCC 6538P, *Bacillus subtilis* ATCC 6633, *Enterococcus faecalis* ATCC 19433, *Escherichia coli* ATCC 7839, *Pseudomonas aeruginosa* ATCC 27853, *Klebsiella pneumoniae* ATCC 13883, and *Candida albicans* ATCC 10231 were obtained from the applied microbiology laboratory, Ferhat Abbas University, Algeria. SHSY-5Y human neuroblastoma cells (ATCC®, CRL-2266) were obtained from ERFARMA Center, Erciyes University, Turkey.

Bee pollen sampling

Bee pollen samples were provided by the International Api-Phyto Therapy Center - Setif - Algeria, from different Algerian clean lands during the spring of 2019, in sterile plastic containers. The samples were subsequently transported to the laboratory and stored at 4°C until use.

Isolation, purification, and conservation of the A23 strain

All the samples were crushed, air dried at room temperature and heated at 50 °C for 30 minutes in a water bath (Memmert, Germany). One gram from all bee pollen samples was mixed with 0.1 G of calcium carbonate (CaCO₃) and incubated at 28 °C for one week.¹⁹ Then, 1 G of each pre-treated sample was suspended in 9 mL of sterile saline water and diluted to 10⁻². After then, 100 µL of the diluted sample was plated on different media for Actinomycetes isolation, and incubated at 28 °C for approximately 10 days. During the period of incubation, the selected strain was purified using yeast extract-malt extract agar (ISP 2 medium), labeled by the A23 strain and conserved at 4 °C.²⁰

Phenotypic identification of the A23 strain

The primary phenotypic characteristics of the A23 strain were determined via Gram staining, catalase and oxidase tests.^{21,22} In addition, the culture characteristics were described based on the growth intensity, aerial and substrate mycelia, and pigment production on ISP 2 agar medium.²³ Also, carbohydrate assimilation was assessed on minimal growth medium supplemented with the carbon source at a final concentration of 1 %, as described by Shirling and Gottlieb (1966).²⁴ The production of extracellular hydrolytic enzymes (starch hydrolysis, protease and lipolysis) was studied on minimum agar medium added to the substrates at a concentration of 1 %.²⁵ Assignments of the A23 strain at least to the genus level were performed by comparing the results of the phenotypic characterization to those reported in Bergey's Manual of Systematic Bacteriology.²⁶

Genotypic identification of the A23 strain

DNA extraction, 16S rRNA amplification, and electrophoresis

The DNA extraction of the selected strain was carried out by using the GF-1 Nucleic Acid Extraction Kit (Vivantis Technologies, Malaysia). The 16S rRNA amplification was performed by PCR using thermocycler (iCycler Bio-Rad, USA) with the help of two universal primers, 27F and 1492R. This process was repeated for 30 cycles.²⁷ After, the products of PCR were subjected to electrophoresis and subsequently purified by a Clean-Up Kit (Vivantis Technologies, Malaysia).²²

DNA sequencing and bioinformatics analysis

The PCR products were purified and subsequently sequenced by using 3130 Genetic Analyzer (Applied Biosystems®, USA).²² BLAST was used to compare the obtained sequence of the studied strain with 16S rRNA gene sequences of other Actinomycetes in GenBank. MEGA 11 software was used to construct the phylogenetic tree.²⁸

Green synthesis, purification and characterization of silver nanoparticles (AgNPs)

Production and purification of red pigment

Red pigment was produced from the A23 strain by submerged fermentation on ISP 2 broth using an orbital shaker at 180 rpm and 28°C. A week later, the culture broth was centrifuged at 4000 rpm and 4 °C for 10 minutes to remove the mycelia. The supernatant that contained the produced pigment was collected and stored at 4°C.²⁹

Synthesis and purification of AgNPs

Two milliliters of the obtained pigment were filtered through a 0.45 µm syringe filter, and mixed with 18 mL of 1 mM and 5 mM silver nitrate solutions at pH 5, pH 7 and pH 9 using a magnetic hotplate stirrer at 1500 rpm and room temperature for 24 hours in dark conditions.^{9,30} The first part of the nanoparticles suspension was obtained directly and kept at 4 °C for UV-Vis spectrophotometer, Zeta potential and DLS analyses, and further experiments. The second part was centrifuged and washed two times with distilled water at 15000 rpm for 10 min, after which the precipitates were dried at 70 °C for 2 days and subjected to characterization using XRD, FT-IR, FE-SEM, and EDX analyses.³¹

Characterization of synthesized AgNPs

Several techniques have been used to characterize the synthesized AgNPs. The formation of AgNPs was confirmed by the visual observation and Ultraviolet visible spectrophotometry (UV-Vis) (Perkin Elmer, USA).⁹ The hydrodynamic diameter was determined via Dynamic light scattering (DLS) (Malvern, UK). The surface charge was analyzed by Zeta potential (Malvern, UK) analyzer. The presence of functional groups playing a role in the synthesis was determined by FT-IR (Perkin Elmer Spectrum 400, USA) analysis. Crystallization was determined by X-ray diffraction (XRD) (BRUKER AXS D8, Germany) analysis. Morphology and elemental presence determined by field emission scanning electron microscopy (FE-SEM) and Energy-dispersive (EDX) analyses (ZEISS GeminiSEM 500, Germany).³²

Biological activities of synthesized AgNPs

Antimicrobial activity

The first test of antimicrobial activity of the synthesized AgNPs was evaluated using the agar well diffusion method as described by Balouiri *et al.* (2016)³³ against *S. aureus* ATCC 6538P, *B. subtilis* ATCC 6633, *E. faecalis* ATCC 19433, *E. coli* ATCC 7839, *P. aeruginosa* ATCC 27853, *K. pneumoniae* ATCC 13883, and *C. albicans* ATCC 10231. Fresh microbial

suspensions (10^7 cfu mL⁻¹) were prepared and swabbed using sterile cotton swabs on Muller-Hinton agar plates. After that, the wells were made using sterilized micropipette tips, and 100 μ L of synthesized AgNPs were poured into each well. Finally, all plates were kept at room temperature for 30 minutes to diffusion, and subsequently incubated at 37 °C for 24 hours. After incubation, the inhibition zone diameter observed around each well was measured and is expressed in millimeters (mm). Gentamicin discs (Oxoid™) and silver nitrate solutions were used as positive controls; pigment alone and distilled water were used as negative controls. After, minimum inhibitory concentrations (MICs) and minimum bactericidal concentrations (MBCs) of AgNPs (5 mM, pH 9) were determined by microbroth dilution method using tetrazolium salts (TTC) in 96 well microplates in triplicate, and on Mueller-Hinton agar plates, respectively.⁹

Anticancer and neuroprotective activities

Final concentrations of 2, 4, 8, 12, and 16 μ g mL⁻¹ of synthesized AgNPs were prepared to use in the evaluation of cytotoxicity and neuroprotective effects on the SHSY-5Y neuroblastoma cells by using the MTT test.

Cytotoxicity assay

After the preparation of SHSY-5Y cells, were exposed to all prepared concentrations of AgNPs for 24 hours in 96 well plates contains approximately 10^4 cells per well. Then, 100 μ L of prepared MTT solution was added to each well, and incubated at 37 °C for 4 hours. Afterwards, the supernatant portion was subsequently removed from the wells, followed by the addition of 100 μ L of DMSO to each well in order to dissolve the MTT salts. Finally, the microplate reader (BioTek, Synergy HT, USA) was used to measure the absorbances at a wavelength of 560 nm.³¹

Neuroprotective activity

To evaluate the potential neuroprotective effects of the synthesized nanoparticles on neuroblastoma cells, the prepared concentrations of AgNPs compounds were added 1 hour after the treatment of cells by H₂O₂ (300 μ M) in 96 well plates. Cell viability was measured by the MTT test after 24 hours of incubation. The same volume of medium without AgNPs or H₂O₂ was used as a control.³¹

Statistical analysis

Data analysis was performed using GraphPad Prism 8.0 software by using ANOVA one-way and Dunnett's post-hoc tests. All differences were considered significant when $P < 0.05$. The n value was four for the cell culture studies.

RESULTS AND DISCUSSION

Phenotypic and genotypic identification of the isolated strain (A23)

As shown in Figure 1, the isolated strain in our study was characterized by earthy odour and powdery colonies with a grey white colour, and it was a filamentous, branching and gram-positive bacterium. Morphological and cultural properties have shown abundant growth with variations in the colour of aerial and substrate mycelia. Additionally, it has the potential to produce a diffusible red pigment. Actinomycetes can produce visible powdery colonies with different colors from the 3rd to 7th day, with an earthy odour as a result of these bacteria's ability to produce various secondary metabolites, including pigments.³⁴

Furthermore, the strain can utilize different carbon sources for growth, and it is also positive for catalase and negative for the oxidase reactions. Protease, lipase, and amylase are produced by this strain (Table I). With the help of Bergey's manual of systematic bacteriology, these phenotypic properties are consistent with the typical characteristics described for the genus *Streptomyces*.²⁶

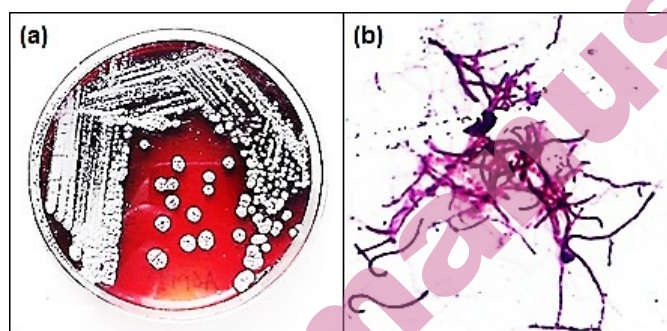


Fig 1 *Streptomyces* sp. A23 strain **a)** Colony morphology **b)** Gram staining

Table I. The phenotypic characteristics of the isolated strain (*Streptomyces* sp. A23)

Morphological and cultural characteristics	
Growth intensity on ISP2 agar	+++
Aerial mycelium colour on ISP2 agar	Grey white
Substrate mycelium colour on ISP2 agar	Dark red
Diffusible pigment	+++
Gram staining	Positive
Carbon sources assimilation	
Glucose	+
Fructose	+
Lactose	+
Maltose	+
Galactose	+
Mannitol	+
Enzymes production	
Catalase	+
Oxidase	-
Starch hydrolysis	+
Casein hydrolysis	+
Lipolysis	+

(⁺) positive reaction; (⁻) negative reaction; (++) elevated production

According to the obtained 16S rRNA sequence (1096 bp) and the phylogenetic tree analyses (Figure 2), the A23 strain belongs to the genus *Streptomyces*. It was labeled *Streptomyces* sp. A23 strain and registered in GenBank under the accession number OR236137.1.

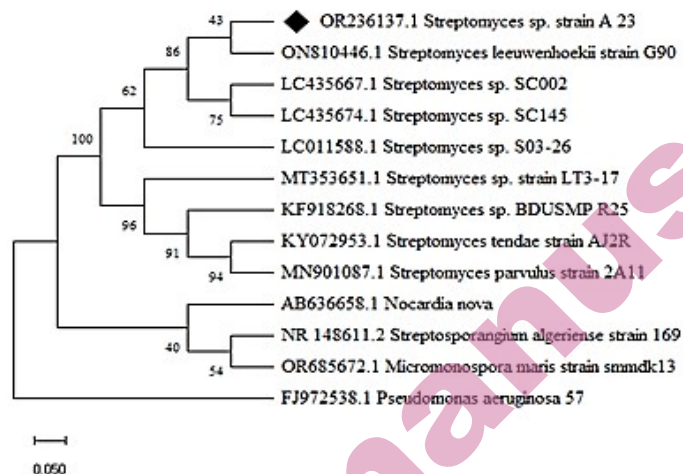


Fig 2 Phylogenetic tree of the *Streptomyces* sp. A23 strain

Green synthesis and characterization of AgNPs

AgNPs were successfully synthesized via a rapid, easy, and eco-friendly procedure using the red pigment of the *Streptomyces* sp. A23 strain that isolated from bee pollen as a bio-reducing agent source. Silver nitrate (AgNO_3) is a colourless solution, and the pigment is red colour. When the pigment was mixed with silver nitrate solution, the mixture slowly turned to the brown colour after 24 hours in the dark (Figure 3). The colour change was due to silver nitrate interacting with the pigment compounds and being bio-reduced from silver nitrate (AgNO_3) to elemental silver (Ag^0). These elementals aggregate to form stable AgNPs.³⁵ A previous study indicated the formation of AgNPs using a pink pigment produced from *Streptomyces* sp. NS-05 isolated from a rhizospheric soil by observing the change in colour to brown.⁸

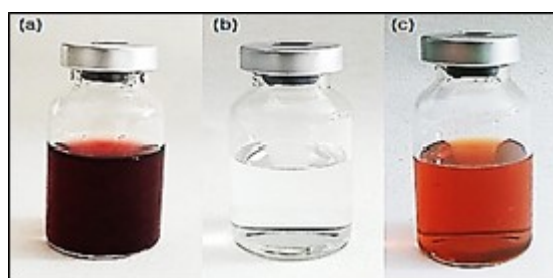


Fig 3 Visual observation of synthesized AgNPs a) Pigment b) AgNO_3 solution c) AgNPs suspensions

In this study, the light absorption points, hydrodynamic diameter, surface charge, crystallization, phytochemical component, morphology and elemental presence of synthesized AgNPs (5 mM, pH 9) were determined by UV-vis, DLS, Zeta potential, XRD, FT-IR, FE-SEM, and EDX analyses, respectively. The optical and electrical properties of nanoparticles are interrelated, and unlike those of their bulk forms, they have a UV-Vis absorption band called surface plasmon resonance (SPR).

UV-vis spectroscopy was used for characterizing the nanoparticles synthesized by various methods. Diffractions observed by analysis can be controlled by many factors, such as reducing agents and solvents.³⁶ According to our results, the characteristic light absorption bands detected at 278 nm and 433 nm by UV-vis analysis were associated with the presence of biomolecules in the pigment and AgNPs, respectively (Figure 4). The characteristic light absorption bands of AgNPs synthesized by using the secondary metabolites of *Streptomyces rochei* and marine *Streptomyces* sp. were measured at 413 and 434 nm, respectively.^{37,38} The structural properties of nanoparticles which depend on the synthesis conditions, also affect the UV-vis characterization bands.³⁹

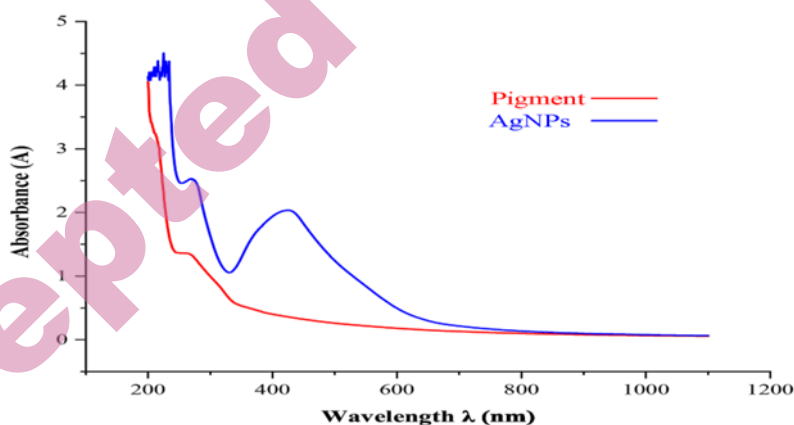


Fig 4 UV-vis spectrum of AgNPs (5 mM, pH 9)

The surface charge of nanoparticles determines the distribution properties of particles, the adsorption properties of ions, and molecules is an important parameter for the characterization of nanomaterials.⁴⁰ The surface charge of the AgNPs synthesized in our study was determined to be -33 mV (Figure 5). A relatively low zeta potential increases the electrostatic repulsion force between nanoparticles, which prevents their aggregation and ensures their stabilization.⁴¹ The surface charge (negative, positive or neutral) of nanoparticles is related to the functional groups on the surface structure.⁴²

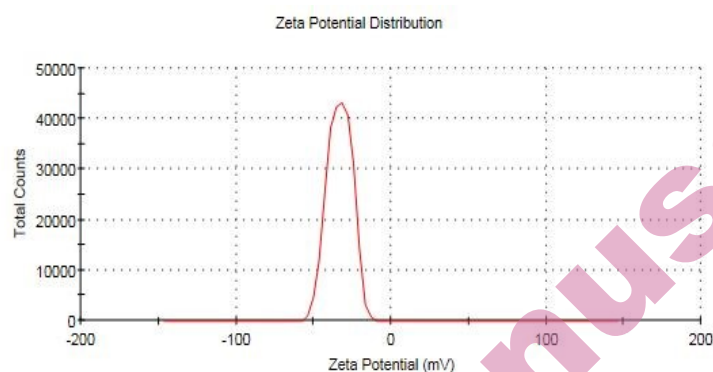


Fig 5 Zeta potential analysis of AgNPs (5 mM, pH 9)

Dynamic light scattering (DLS) is a spectroscopic analysis technique used to determine the size of particles suspended in a liquid from 1 to 1000 nm.⁴³ The average hydrodynamic size of our synthesized AgNPs was 112 nm (Figure 6). DLS measurements are expected to yield more intense results than microscopic analyses, which can be explained by the presence of ions or molecules bound, and the increase in the thickness of the hydration shell around nanoparticles in solution.^{44,45}

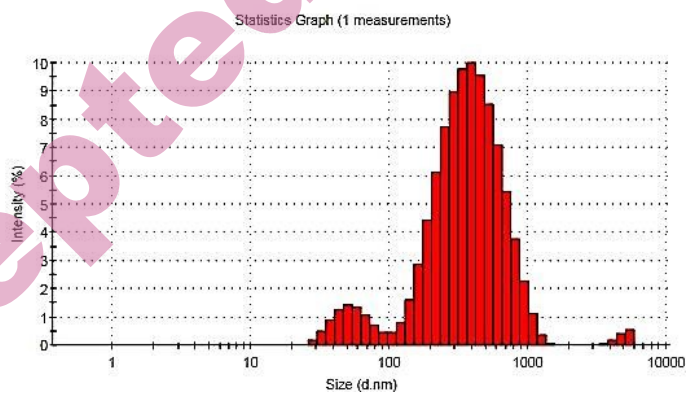


Fig 6 DLS analysis of AgNPs (5 mM, pH 9)

According to the FE-SEM image, our synthesized spherical AgNPs tend to form agglomerations and appear to be monodispersed with a mean particle size of 54.5 nm (Figure 7). The average size of the spherical AgNPs synthesized by using the pink pigment of *Streptomyces* sp. NS-05 was 42.5 nm.⁸ The size, shape, and structural properties of NPs synthesized by biological methods can vary depending on the biological agent used and the synthesis conditions, such as the concentration and type of metal salt used and the bio-reducing agent, temperature and reaction time.⁴⁶

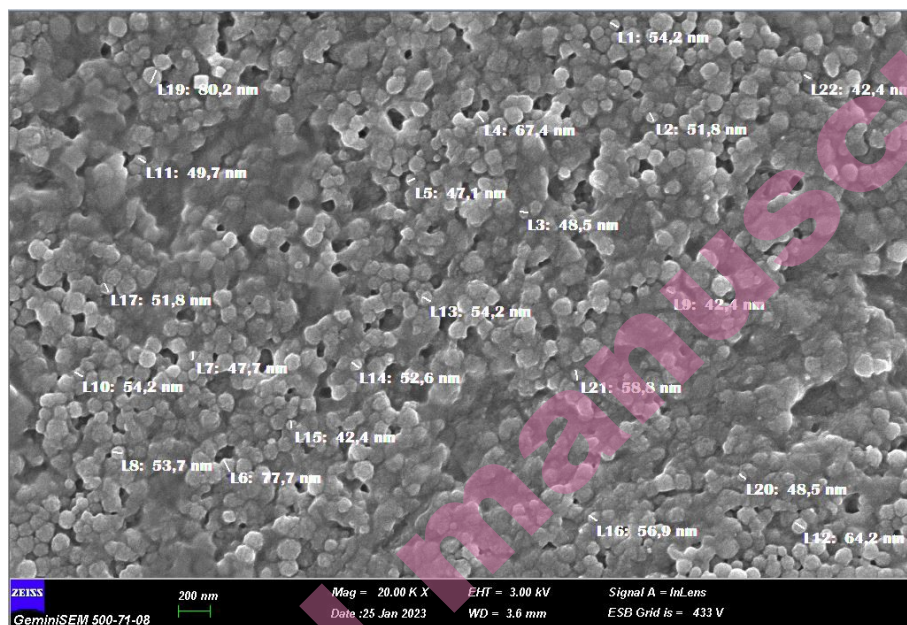


Fig 7 FE-SEM image of AgNPs (5 mM, pH 9)

EDX and XRD were performed to determine the elemental composition and crystal structure of the AgNPs. The presence of Ag was revealed by EDX analysis (Figure 8).

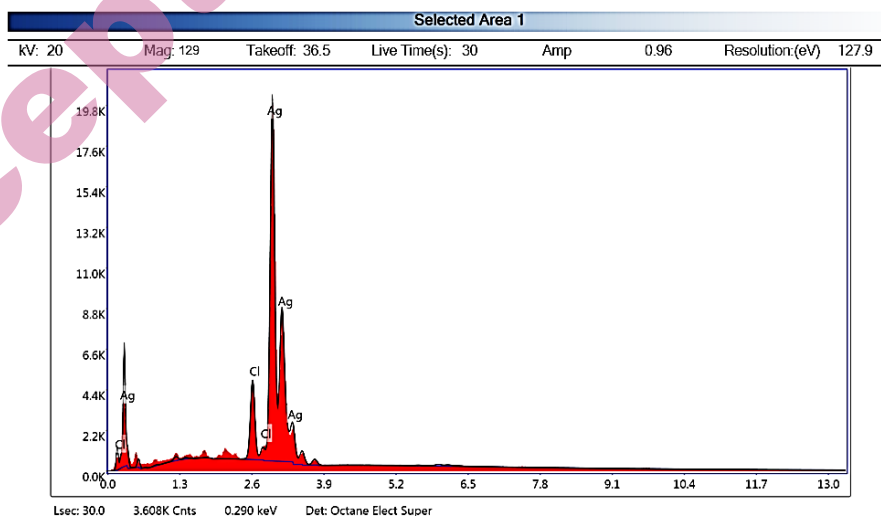


Fig 8 EDX analysis of AgNPs (5 mM, pH 9)

According to the XRD analysis of the Ag/Ag⁰ NPs, the 27.7°, 32.3°, 38.4°, 44.1°, 46.2°, 54.5°, 57.6°, 64.3° and 77.2° peaks observed at 2 theta corresponded to the (1, 0, 0), (1, 2, 2), (1, 1, 1), (2, 0, 0), (2, 0, 0), (2, 2, 0), (2, 2, 0), (2, 2, 0), and (3, 1, 1) planes, respectively (Figure 9). The obtained peaks at 27.7°, 32.3°, and 54.5° indicate Ag⁰ NPs (JCPDS (01-076-1489)). The peaks at 32.3°, 38.4°, 46.2°, 54.5°, 57.6°, 64.3° and 77.2° reflect the face-centered cubic Ag phase (JCPDS (00-001-1167)).^{47,48,49}

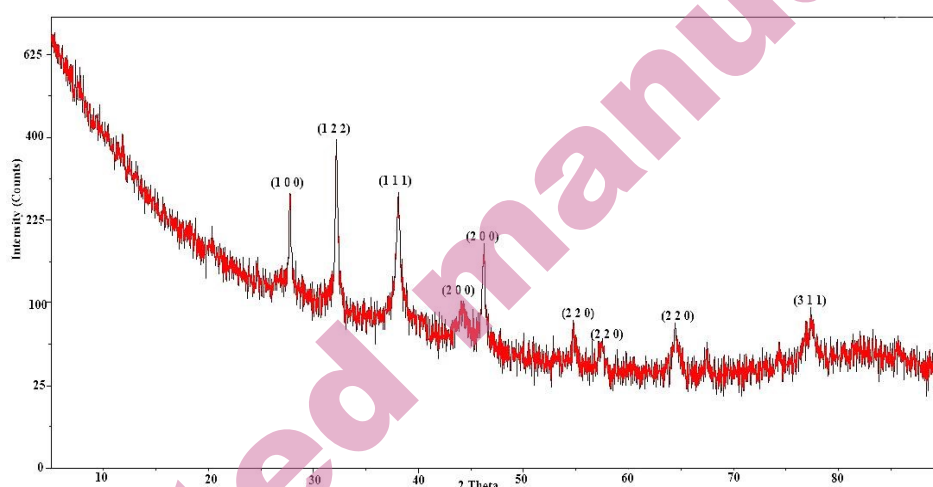


Fig 9 XRD pattern of AgNPs (5 mM, pH 9)

FT-IR can provide information about the bioactive molecules that may be responsible for reducing silver ions into AgNPs.¹² The functional groups that play a role in the green synthesis of our AgNPs were revealed by the peaks observed in the FT-IR spectrum with diffractions at 3471, 2918, 1620, 1409, 1321, and 478 cm⁻¹, which indicate the presence of alcohol (O-H), alkane (C-H), amine (N-H), fluoro compound (C-F), aromatic amine (C-N), and metal (Ag), respectively (Figure 10). Similar to our findings, previous studies reported that alcohol, alkane, and amine groups were responsible for the reduction and capping of Ag ions for the synthesis of NPs.^{11,38,41}

Antimicrobial activity

Firstly, the antimicrobial activity of synthesized nanoparticles (AgNPs) by using the red pigment produced from *Streptomyces* sp. A23 strain was evaluated using an agar well diffusion assay as illustrated in Figure 11.

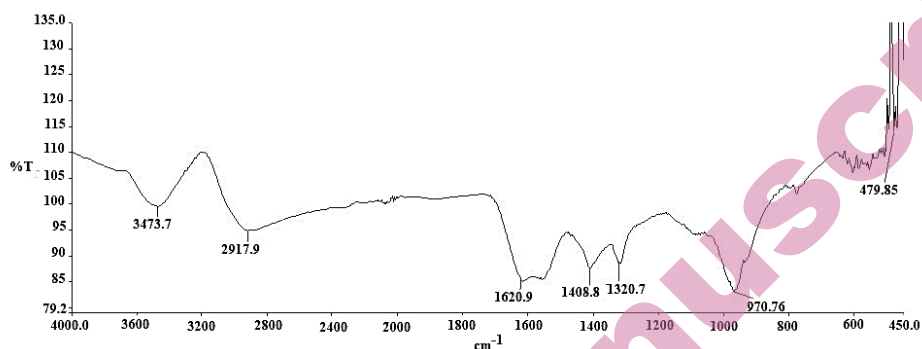


Fig 10 FT-IR spectrum of AgNPs (5 mM, pH 9)

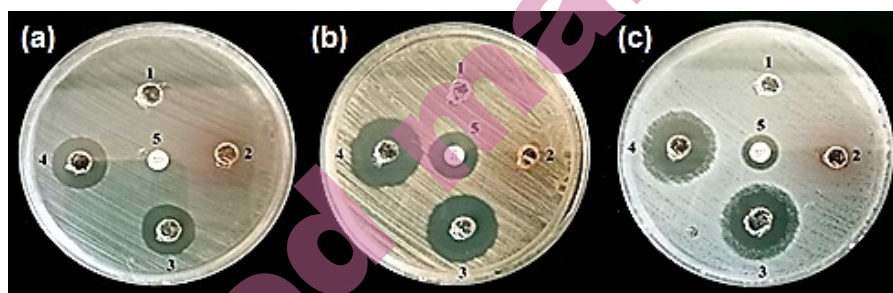


Fig 11 Antimicrobial activity of AgNPs (1 mM, pH 7) against **a)** *E. faecalis* **b)** *S. aureus* **c)** *P. aeruginosa* **1)** H₂O **2)** Pigment **3)** AgNO₃ **4)** AgNPs **5)** Gentamicin

The obtained results showed that AgNPs (5 mM, pH 9) demonstrated the best antimicrobial effect against the tested pathogenic microorganisms (Table II). The zone with greatest diameter of inhibition was observed for *E. faecalis* ATCC 19433 (32 mm), followed by *S. aureus* ATCC 6538P (30 mm), *C. albicans* ATCC 10231 (30 mm), *P. aeruginosa* ATCC 27853 (27 mm), *B. subtilis* ATCC 6633 (25 mm), *K. pneumoniae* ATCC 13883 (20 mm), and *E. coli* ATCC 7839 (19 mm). The AgNPs synthesized by using the secondary metabolites of *Streptomyces hirsutus* isolated from Indian sediment samples exhibited significant effects against *E. faecalis*, *S. aureus*, *E. coli*, *P. aeruginosa*, and *C. albicans* with inhibition zones of 21, 19, 17, 12 and 12 mm, respectively.⁷

AgNPs (5 mM, pH 9) are more effective because of their spherical shape and smaller size (51 nm), and their contact with microbial surfaces is good and easy due to their high negative surface charge (-33 mV). According to different reports, physical properties such as size, shape, and surface charge can influence the antimicrobial activity.⁵⁰⁻⁵² In addition, many previous studies have shown that one of the critical characteristics of nanoparticles is size, and a smaller size has a higher effect on the ability of nanoparticles to penetrate into microbial cells.⁵² Additionally, the shape of AgNPs plays an important role in the antimicrobial

activity, and it was decided that a spherical shape would result in excellent activity.⁵³ Furthermore, the surface charge plays a crucial role in the initial adsorption of nanoparticles to cell membranes.⁵¹

Table II. Antimicrobial activity of synthesized AgNPs

Pathogenic microorganisms	Inhibition zones diameter (mm)					
	AgNPs				Controls	
	(1 mM, pH5)	(1 mM, pH7)	(5 mM, pH9)	AgNO ₃ (1 mM)	Pigment	Gentamicin (10 µg)
<i>S. aureus</i> ATCC 6538P	21	24	30	22	00	17
<i>B. subtilis</i> ATCC 6633	22	16	25	15	00	14
<i>E. faecalis</i> ATCC 19433	25	18	32	16	00	-
<i>E. coli</i> ATCC 7839	18	21	19	20	00	14
<i>P. aeruginosa</i> ATCC 27853	23	23	27	23	00	12
<i>K. pneumoniae</i> ATCC 13883	20	26	20	24	00	14
<i>C. albicans</i> ATCC 10231	27	28	30	33	11	-

(ATCC) American type culture collection

For the MICs and MBCs of AgNPs (5 mM, pH 9), we recorded the lowest MIC against *S. aureus* ATCC 6538P and *B. subtilis* ATCC 6633 with a value amounted by 62.5 µg mL⁻¹, while the highest MIC was against *P. aeruginosa* ATCC 27853 (250 µg mL⁻¹). The lowest MBC (62.5 µg mL⁻¹) was recorded against *B. subtilis* ATCC 6633, while the highest MBC (>1000 µg mL⁻¹) was against *P. aeruginosa* ATCC 27853 (Table III). The minimum inhibitory concentration (MIC) value is the lowest concentration of the tested substance as an antibiotic that inhibits the growth of the test microorganisms after an overnight of incubation, while the minimum bactericidal concentration (MBC) value is the lowest concentration required to kill 99.9% of the test microorganisms.^{7,9}

Table III. MICs and MBCs results of AgNPs (5 mM, pH 9)

Pathogenic microorganisms	MIC (µg mL ⁻¹)	MBC (µg mL ⁻¹)
<i>S. aureus</i> ATCC 6538P	62.5	125
<i>B. subtilis</i> ATCC 6633	62.5	62.5
<i>E. coli</i> ATCC 7839	125	125
<i>P. aeruginosa</i> ATCC 27853	250	> 1000
<i>K. pneumoniae</i> ATCC 13883	125	125

(ATCC) American type culture collection

There is no clear or exact mechanism for the antimicrobial effect of AgNPs, but many existing studies have reported that the most common and prominent mechanisms are as follows: a) AgNPs can adhere to the cell wall and membrane of microbial cells, causing cell rupture and leading to cell lysis. b) AgNPs can penetrate the inside of microbial cells and damage biomolecules (DNA and enzymes) and intracellular structures (mitochondria, vacuoles and ribosomes). c) AgNPs have the potential to increase ROS production, which can cause oxidative stress and damage to microbial cells.^{54,55}

Anticancer and neuroprotective activities

In the MTT test, SH-SY5Y cells were treated with various concentrations of AgNPs to determine their cytotoxic effects (Figure 12). Compound-1 (AgNPs, 1 mM, pH 5) did not alter cell viability at concentrations of 2 or 4 $\mu\text{g mL}^{-1}$, but at concentrations of 8, 12 and 16 $\mu\text{g mL}^{-1}$ ($p < 0.001$), it significantly reduced cell viability compared to that of the control group. For compound-2 (AgNPs, 1 mM, pH 7), a concentration of 2 $\mu\text{g mL}^{-1}$ tended to increase cell viability, but this increase was not statistically significant. Additionally, there was no change in the cell viability at 4 $\mu\text{g mL}^{-1}$. Also, at concentrations of 8, 12 and 16 $\mu\text{g mL}^{-1}$ ($p < 0.001$), the cell viability was markedly lower than that in the control group. Compound-3 (AgNPs, 5 mM, pH 9) significantly decreased ($p < 0.001$) cell viability at concentrations of 2, 4, 8, 12 and 16 $\mu\text{g mL}^{-1}$ compared to that of the control.

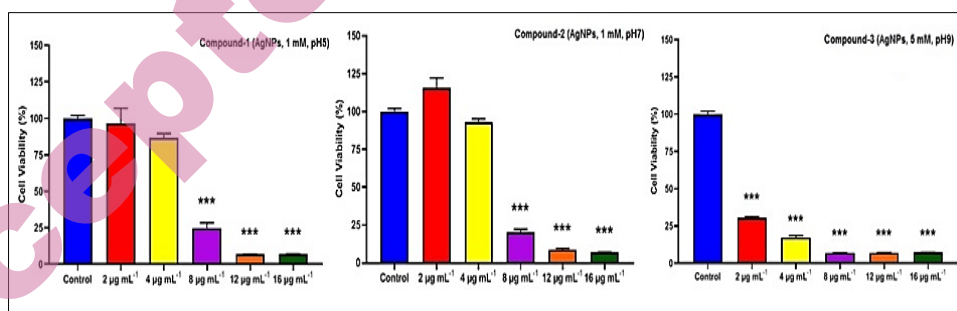


Fig 12 Effects of synthesized AgNPs on the viability of SH-SY5Y cells ***: $p < 0.001$ compared to the control

For the neuroprotective activity, MTT assay was performed to determine the neurotoxic dose of H_2O_2 as shown in Figure 13. Treatment with 100, 150, 200, 300, 400 and 600 μM of H_2O_2 reduced ($p < 0.001$) cell viability compared to that of the control group. To evaluate the neuroprotective effect of synthesized nanoparticles, 300 μM H_2O_2 was added one hour before the AgNPs were added, and cell viability was investigated via the MTT test at the 24th hour of AgNPs treatment. When the neuroprotective effects of the AgNPs were examined, compound-1 (AgNPs, 1

mM, pH 5) at concentrations of 2, 4, 8, 12 and 16 $\mu\text{g mL}^{-1}$ ($p < 0.001$) significantly reduced the viability of the SH-SY5Y cells compared to that of the H_2O_2 group. Compound-2 (AgNPs, 1 mM, pH 7) at a concentration of 2 $\mu\text{g mL}^{-1}$ ($p < 0.01$) significantly increased the cell viability with the presence of H_2O_2 . In addition, at concentrations of 8, 12 and 16 $\mu\text{g mL}^{-1}$ ($p < 0.001$), the cell viability was markedly lower than that in the H_2O_2 group. Treatment with compound-3 (AgNPs, 5 mM, pH 9) at concentrations of 2, 4, 8, 12 and 16 $\mu\text{g mL}^{-1}$ ($p < 0.001$) significantly reduced the viability of the SH-SY5Y cells compared to that of the H_2O_2 group.

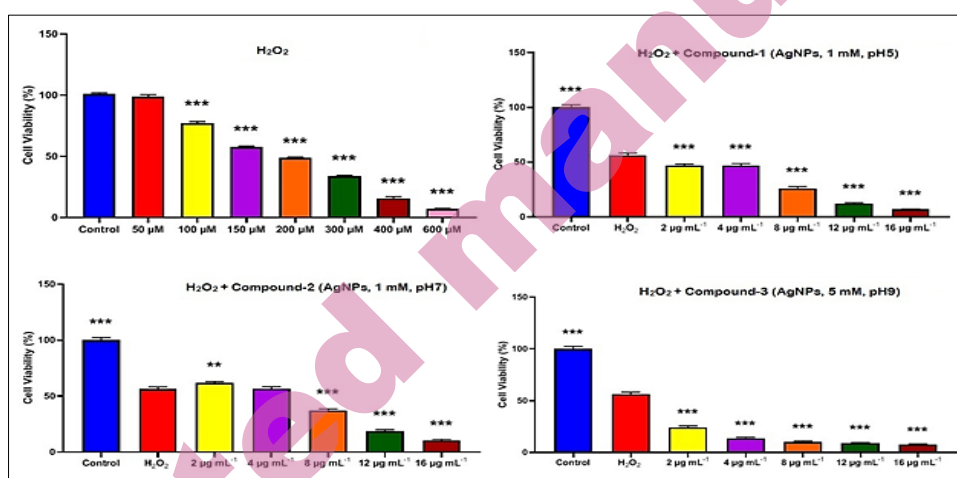


Fig 13 Neuroprotective activity of synthesized AgNPs **: $p < 0.01$ ***: $p < 0.001$ compared to the control group

In this study, cell culture experiments were conducted to address two primary objectives concerning SH-SY5Y neuroblastoma cells. First, the anticancer activity of synthesized AgNPs was investigated by assessing their cytotoxic effects on neuroblastoma cells. Determination of the optimal cytotoxic dose was crucial for evaluating the anticancer potency of the synthesized materials. Notably, Compound-1, Compound-2, and Compound-3 exhibited cytotoxic effects at concentrations of 2, 4, and 8 $\mu\text{g mL}^{-1}$, respectively. Comparative analysis revealed the superior anticancer activity of compound-3 against neuroblastoma cells. This observation aligns with recent studies, confirming the anticancer efficacy of silver nanoparticles synthesized by using bioactive molecules produced by some *Streptomyces* strains on different cancer cell lines.^{7,39} Additionally, our study was the first to show that AgNPs synthesized using a red pigment of *Streptomyces* sp. had anticancer activities on human neuroblastoma cells, although there are several studies showing anticancer and cytotoxic effects of different source-based AgNPs.^{56,57}

The second objective focused on elucidating the potential neuroprotective effects of AgNPs against hydrogen peroxide-induced cytotoxicity, a common mechanism underlying neurodegenerative diseases. Hydrogen peroxide (H₂O₂) at a concentration of 100 µM demonstrated cytotoxic effects, and a concentration of 300 µM was selected for its moderate cytotoxic effects, as suggested by prior study.⁵⁸ Intriguingly, compound-2 exhibited neuroprotective effects at the lowest concentration tested, distinguishing it from the other compounds. The observed neuroprotective effects of compound-2 were hypothesized to be associated with its potential antioxidant properties, drawing parallels with findings from Alkhalaf et al. in 2020,⁵⁹ who demonstrated that the antioxidant and anti-inflammatory effects of AgNPs synthesized by using *Nigella sativa* extract in rodents. Controversially, Zhai et al. (2022) showed the cytotoxic effects of AgNPs via oxidative stress mechanism in SH-SY5Y cells. It has been seen that AgNPs oxidative stress at very high doses (40 and 60 µg mL⁻¹), whereas we observed the neuroprotective effect of low doses of AgNPs (2 and 4 µg mL⁻¹) against a well-known oxidative stressor, H₂O₂, in our study. These differences suggest a dose-dependent antioxidant or oxidant effect of AgNPs synthesized using the red pigment produced by the *Streptomyces* sp. A23 strain.⁵⁷ These findings suggested a nuanced interplay between antioxidant effects at lower concentrations and antiproliferative effects at higher concentrations for the compound-2.

CONCLUSION

In conclusion, the green synthesis of silver nanoparticles (AgNPs) using the red pigment produced by the *Streptomyces* sp. A23 strain isolated from Algerian bee pollen represents a new approach with remarkable neuroprotective, anticancer and antimicrobial activities. This synthesis method not only harnesses the inherent capabilities of the *Streptomyces* sp. A23 strain but also produces silver nanoparticles with unique biological properties, paving the way for their application in diverse therapeutic avenues. Future studies should address the molecular mechanisms underlying the therapeutic properties of these nanoparticles, including the molecular interactions between the AgNPs and biological targets, which will also provide deeper insight into their mode of action. Additionally, the exploration of synergistic effects with other therapeutic agents could open new possibilities for enhanced treatment strategies, especially in multidrug-resistant infections and complex diseases like cancer and neurodegeneration.

Acknowledgements: This study was supported by the Directorate-General for Scientific Research and Technological Development of Algeria (DGRSDT). The authors are grateful to Alla Koudieh - Manager of the International Api-Phyto Therapy Center, Setif, Algeria - who has helped this research.

ИЗВОД

ОДРЕЂИВАЊЕ АНТИМИКРОБНЕ, АНТИКАНЦЕРСКЕ И НЕУРОПРОТЕКТИВНЕ АКТИВНОСТИ НАНОЧЕСТИЦА СРЕБРА (AgNP) СИНТЕТИСАНИХ ПРИМЕНОМ ЗЕЛЕНЕ ХЕМИЈЕ КОРИСТЕЊИ ЦРВЕНИ ПИГМЕНТ СОЈА *STREPTOMYCES* SP. A23 ИЗОЛОВАНОГ ИЗ АЛЖИРСКОГ ПЧЕЛИЊЕГ ПОЛЕНА

МОКНАСНЕ МОХАМЕД¹, БЕЛХАДЖ ХАНИ¹, ФАТИХ ДОГАН КОСА², ГОКХАН УНАЛ³, НАСРАТ АБДУЛ РАХМАН⁴, АЈСЕГУЛ ВАСМА², НУН МЕХМЕТ БОЗКУРТ³, АХМЕД АЛИЕН МОХАМЕД БАШИР¹ И ХАРЗАЛЛАХ ДАОУД¹

¹Applied Microbiology Laboratory, Natural Sciences and Life Faculty, Ferhat Abbas Setif 1 University, Setif, 19137, Algeria, ²Aquatic Animals and Diseases Laboratory, Veterinary Medicine Faculty, Erciyes University, Talas, 38280, Kayseri, Turkey, ³Pharmacology Department, Pharmacy Faculty, Erciyes University, Talas, 38280, Kayseri, Turkey u ⁴Institute of Natural and Applied Science, Erciyes University, Talas, 38280, Kayseri, Turkey.

Црвени пигмент из соја *Streptomyces* sp. A23 изолован из алжирског пчелињег полена је коришћен за синтезу наночестица сребра (AgNP) применом зелене хемије, а затим је одређивана њихова антимикробна, антиканцерска и неуропротективна активност. AgNP су синтетисане редукцијом 1 mM и 5 mM раствора сребро нитрата на различитим pH (5, 7 и 9), а затим окарактерисане. AgNP (5 mM, pH 9) су испољиле максимум UV-vis апсорбанце на 433 nm. Методом DLS је утврђено да је просечни пречник честица 112 nm. Максимум зета потенцијала је утврђен на -33 mV, потврђујући повећану стабилност. XRD анализом је констатована кристална природа материјала. FT-IR анализом су утврђене специфичне функционалне групе на положају 3471 cm⁻¹ до 478 cm⁻¹. FE-SEM методом је показано да је средња вредност пречника сферних AgNP 54,5 nm. Присуство Ag је потврђено EDX анализом. Наночестице су испољиле значајну антимикробну активност спрам *E. faecalis* ATCC 19433, *C. albicans* ATCC 10231, *S. aureus* ATCC 6538P, *P. aeruginosa* ATCC 27853, *B. subtilis* ATCC 6633, *K. pneumoniae* ATCC 13883 и *E. coli* ATCC 7839, уз зону инхибиције од 32, 30, 30, 27, 25, 20, односно 19 mm. Најниже вредности MIC и MBC су измерене спрам *B. subtilis* ATCC 6633 – 62,5 µg mL⁻¹. Занимљиво је да су све синтетисане AgNP, у концентрацијама 2, 4 и 8 µg mL⁻¹, испољиле цитотоксични ефекат на SH-SY5Y ћелијску линију неуробластома. Додатно, AgNP (1 mM, pH 7) су испољиле значајну неуропротективну активност при најнижим тестираним концентрацијама. Из свега наведеног произилази да се AgNP синтетисане применом црвеног пигмента *Streptomyces* sp. сој A23 могу сагледати као обећавајући терапеутски агенси.

(Примљено 15. септембра 2024; ревидирано 8. октобра 2024; прихваћено 15. јануара 2025.)

REFERENCES

1. S. Malik, K. Muhammad, Y. Waheed, *Molecules* **28** (2023) 6624 (<https://doi.org/10.3390/molecules28186624>)
2. L. Xu, Y. Y. Wang, J. Huang, C. Y. Chen, Z. X. Wang, H. Xie, *Theranostics* **10**(20) (2020) 8996 (<https://doi.org/10.7150/thno.45413>)
3. A. Dhaka, S. C. Mali, S. Sharma, R. Trivedi, *Results Chem.* **6** (2023) 1-21 (<https://doi.org/10.1016/j.rechem.2023.101108>)
4. S. Barbuto Ferraiuolo, M. Cammarota, C. Schiraldi, O. F. Restaino, *Appl. Microbiol. Biotechnol.* **105** (2021) 551-568 (<https://doi.org/10.1007/s00253-020-11064-2>)

5. A. Rosyidah, O. Weeranantanapan, N. Chudapongse, W. Limphirat, N. Nantapong, *RSC Adv.* **12** (2022) 4336 (<https://doi.org/10.1039/D1RA08238H>)
6. N. A. Al-Dhabi, A. K. M. Ghilan, M. V. Arasu, V. Duraipandiyan, *J. Photoch. Photob. B: Bio.* **189** (2018) 176-184 (<https://doi.org/10.1016/j.jphotobiol.2018.09.012>)
7. S. S. Pallavi, H. A. Rudayni, A. Bepari, S. K. Niazi, S. Nayaka, *Saudi J. Biol. Sci.* **29** (2022) 228-238 (<https://doi.org/10.1016/j.sjbs.2021.08.084>)
8. N. Singh, B. Naik, V. Kumar, V. Kumar, S. Gupta, *J. Microbiol. Biotech. Food Sci.* **10(4)** (2021) 604-608 (<https://doi.org/10.15414/jmbfs.2021.10.4.604-608>)
9. M. S. Mechouche, F. Merouane, C. E. H. Messaad, N. Golzadeh, Y. Vasseghian, M. Berkani, *Environ. Res.* **204** (2022) 1-14 (<https://doi.org/10.1016/j.envres.2021.112360>)
10. K. D. Datkhile, S. Chakraborty, P. P. Durgawale, S. R. Patil, *Pharm. Nanotechnol.* **12(4)** (2024) 340-350 (<https://doi.org/10.2174/2211738511666230913095001>)
11. C. Ghosh, P. Sarkar, R. Issa, J. Haldar, *Trends Microbiol.* **27(4)** (2019) 323-338 (<https://doi.org/10.1016/j.tim.2018.12.010>)
12. H. M. Abd-Elhady, M. A. Ashor, A. Hazem, F. M. Saleh, S. Selim, N. El Nahhas, S. H. Abdel-Haféz, S. Sayed, E. A. Hassan, *Molecules* **27** (2022) 1-14 (<https://doi.org/10.3390/molecules27010212>)
13. K. Aabed, A. E. Mohammed, *Front. Bioeng. Biotechnol.* **9** (2021) 1-14 (<https://doi.org/10.3389/fbioe.2021.652362>)
14. K. Kopeć, S. Szleszkowski, D. Koziorowski, S. Szlufik, *Int. J. Mol. Sci.* **24** (2023) 1-18 (<https://doi.org/10.3390/ijms241210366>)
15. M. Xu, X. Han, H. Xiong, Y. Gao, B. Xu, G. Zhu, J. Li, *Molecules* **28** (2023) 1-20 (<https://doi.org/10.3390/molecules28135145>)
16. F. E. Salem, H. M. Yehia, S. M. Korany, K. M. Alarjani, A. H. Al-Masoud, M. F. Elkhadragey, *Food Sci. Technol.* **42** (2022) 1-12 (<https://doi.org/10.1590/fst.97322>)
17. J. Baranwal, B. Barse, A. Di Petrillo, G. Gatto, L. Pilia, A. Kumar, *Materials* **16** (2023) 1-24 (<https://doi.org/10.3390/ma16155354>)
18. F. D. Zhu, Y. J. Hu, L. Yu, X. G. Zhou, J. M. Wu, Y. Tang, D. L. Qin, Q. Z. Fan, A. G. Wu, *Front. Pharmacol.* **12** (2021) 1-19 (<https://doi.org/10.3389/fphar.2021.683935>)
19. E. Hernández-Bolaños, D. Montesdeoca-Flores, E. Abreu-Yanes, M. L. Barrios, N. Abreu-Acosta, *Curr. Microbiol.* **77** (2020) 2510-2522 (<https://doi.org/10.1007/s00284-020-02030-2>)
20. H. Mohamed, B. Miloud, F. Zohra, J. M. García-Arenzana, A. Veloso, S. Rodríguez-Couto, *Int. J. Mol. Cell. Med.* **6(2)** (2017) 109-120 (<https://doi.org/10.22088/acadpub.BUMS.6.2.5>)
21. A. C. Smith, M. A. Hussey, *ASM* (2005) 1-9 (<https://asm.org:443/Protocols/Gram-Stain-Protocols>)
22. M. Lakhdar, D. Abir, M. Fatna, *J. Agric. Appl. Bio.* **4(1)** (2023) 71-82 (<https://doi.org/10.11594/jaab.04.01.08>)
23. A. Tandale, M. Khandagale, R. Palaskar, S. Kulkarni, *Int. J. Curr. Res. Life Sci.* **7(6)** (2018) 2397-2402 (<http://www.journalijrls.com/sites/default/files/issues-pdf/01212.pdf>)
24. E. T. Shirling, D. Gottlieb, *Int. J. Syst. Evol. Microbiol.* **16(3)** (1966) 313-340 (<https://doi.org/10.1099/00207713-16-3-313>)

25. M. Mahfooz, S. Dwedi, A. Bhatt, S. Raghuvanshi, M. Bhatt, P. K. Agrawal, *Int. J. Curr. Microbiol. App. Sci.* **6**(7) (2017) 4084-4100 (<https://doi.org/10.20546/ijcmas.2017.607.424>)
26. M. Goodfellow, K. A. Peter, H. J. Busse, M. F. Trujillo, W. Ludwig, K. I. Suzuki, A. Parte, *Bergey's Manual® of Systematic Bacteriology*, Springer, New York, USA, 2012 (<https://doi.org/10.1007/978-0-387-68233-4>)
27. F. Z. Djebbah, N. A. Al-Dhabi, M. V. Arasu, L. Belyagoubi, F. Kherbouche, D. E. Abdelouahid, B. Ravindran, *J. King Saud Univ. Sci.* **34** (2022) 101719 (<https://doi.org/10.1016/j.jksus.2021.101719>)
28. M. S. Almuhayawi, M. S. Mohamed, M. Abdel-Mawgoud, S. Selim, S. K. Al Jaouni, H. AbdElgawad, *Biology* **10** (2021) 1-22 (<https://doi.org/10.3390/biology10030235>)
29. T. Nuanjohn, N. Suphrom, N. Nakaew, W. Pathom-Aree, N. Pensupa, A. Siangsuepchart, J. Jumpathong, *Molecules* **28** (2023) 1-18 (<https://doi.org/10.3390/molecules28165949>)
30. N. K. Ahila, V. S. Ramkumar, S. Prakash, B. Manikandan, J. Ravindran, P. K. Dhanalakshmi, E. Kannapiran, *Biomed. Pharmacother.* **84** (2016) 60-70 (<https://doi.org/10.1016/j.biopha.2016.09.004>)
31. F. D. Koca, M. G. Halici, Y. Işık, G. Ünal, *Inorg. Nano-Met. Chem.* (2022) 1-8 (<https://doi.org/10.1080/24701556.2022.2078351>)
32. A. K. Shukla, S. Iravani, *Green Synthesis, Characterization and Applications of Nanoparticles*, Elsevier, Amsterdam, Netherlands, 2019 (<https://doi.org/10.1016/C2017-0-02526-0>)
33. M. Balouiri, M. Sadiki, S. K. Ibnouda, *J. Pharm. Anal.* **6** (2016) 71-79 (<https://doi.org/10.1016/j.jpha.2015.11.005>)
34. M. Abou-Dobara, M. Mousa, M. Hasaneen, S. Nabih, *J. Agric. Chem. Biotech.* **9**(12) (2018) 283-287 (<https://doi.org/10.21608/jacb.2018.37039>)
35. S. Jabeen, R. Qureshi, M. Munazir, M. Maqsood, M. Munir, S. H. Shah, B. Z. Rahim, *Mater. Res. Express* **8** (2021) 092001 (<https://doi.org/10.1088/2053-1591/ac1de3>)
36. I. Khan, K. Saeed, I. Khan, *Arab. J. Chem.* **12** (2019) 908-931 (<https://doi.org/10.1016/j.arabjc.2017.05.011>)
37. N. Bano, D. Iqbal, A. Al Othaim, M. Kamal, H. M. Albadrani, N. A. Algehainy, Roohi, *Sci. Rep.* **13** (2023) 4150 (<https://doi.org/10.1038/s41598-023-30215-9>)
38. K. Kamala, G. J. J. Kumar, D. Ganapathy, A. K. Sundramoorthy, P. Sivaperumal, *Curr. Anal. Chem.* **19** (2023) 550-560 (<https://doi.org/10.2174/0115734110262574230927045451>)
39. M. Asif, R. Yasmin, R. Asif, A. Ambreen, M. Mustafa, S. Umbreen, *Dose-Response* **20** (2022) 1-11 (<https://doi.org/10.1177/15593258221088709>)
40. S. Mourdikoudis, R. M. Pallares, N. T. Thanh, *Nanoscale* **10** (2018) 12871-12934 (<https://doi.org/10.1039/C8NR02278J>)
41. T. Varadavenkatesan, R. Selvaraj, R. Vinayagam, *Mater. Today: Proc.* **23** (2020) 39-42 (<https://doi.org/10.1016/j.matpr.2019.05.441>)
42. M. Awashra, P. Młynarz, *Nanoscale Adv.* **5** (2023) 2674-2723 (<https://doi.org/10.1039/D2NA00534D>)
43. Z. Jia, J. Li, L. Gao, D. Yang, A. Kanaev, *Colloids Interfaces* **7** (2023) 1-18 (<https://doi.org/10.3390/colloids7010015>)
44. Z. Gharari, P. Hanachi, H. Sadeghinia, T. R. Walker, *Pharmaceuticals* **16** (2023) 1-20 (<https://doi.org/10.3390/ph16070992>)

45. M. H. Moosavy, M. Guardia, A. Mokhtarzadeh, S. A. Khatibi, N. Hosseinzadeh, N. Hajipour, *Sci. Rep.* **13** (2023) 7230 (<https://doi.org/10.1038/s41598-023-33632-y>)
46. N. Kizildag, S. Cenkseven, F. D. Koca, H. Aka Sagliker, C. Darici, *Eur. J. Soil Biol.* **91** (2019) 18-24 (<https://doi.org/10.1016/j.ejsobi.2019.01.001>)
47. H. Fouad, G. Yang, A. A. El-Sayed, G. Mao, D. Khalafallah, M. Saad, H. Ga'al, E. Ibrahim, J. Mo, *J. Nanobiotechnol.* **19** (2021) 1-17 (<https://doi.org/10.1186/s12951-021-01068-z>)
48. I. A. M. Ali, A. B. Ahmed, H. I. Al-Ahmed, *Sci. Rep.* **13** (2023) 2256 (<https://doi.org/10.1038/s41598-023-29412-3>)
49. S. Korpayev, H. Hamrayev, N. Aničić, U. Gašić, G. Zengin, M. Agamyradov, G. Agamyradova, H. Rozyyev, G. Amanov, *Biomass Convers. Biorefin.* **14**(19) (2024) 24715-24729 (<https://doi.org/10.1007/s13399-023-04648-1>)
50. K. Kalwar, D. Shan, *Micro Nano Lett.* **13**(3) (2018) 277-280 (<https://doi.org/10.1049/mnl.2017.0648>)
51. M. K. Rasmussen, J. N. Pedersen, R. Marie, *Nat. Commun.* **11** (2020) 1-8 (<https://doi.org/10.1038/s41467-020-15889-3>)
52. P. R. More, S. Pandit, A. D. Filippis, G. Franci, I. Mijakovic, M. Galdiero, *Microorganisms* **11** (2023) 1-27 (<https://doi.org/10.3390/microorganisms11020369>)
53. A. Menichetti, A. Mavridi-Printezi, D. Mordini, M. Montalti, *J. Funct. Biomater.* **14** (2023) 1-21 (<https://doi.org/10.3390/jfb14050244>)
54. T. C. Dakal, A. Kumar, R. S. Majumdar, V. Yadav, *Front. Microbiol.* **7** (2016) 1-17 (<https://doi.org/10.3389/fmicb.2016.01831>)
55. A. Roy, O. Bulut, S. Some, A. K. Mandal, M. D. Yilmaz, *RSC Adv.* **9** (2019) 2673-2702 (<https://doi.org/10.1039/C8RA08982E>)
56. Y. Shkryl, T. Rusapetova, Y. Yugay, A. Egorova, V. Silant'ev, V. Grigorchuk, A. Karabtsov, Y. Timofeeva, E. Vasyutkina, O. Kudinova, V. Ivanov, V. Kumeiko, V. Bulgakov, *Int. J. Mol. Sci.* **22**(7) (2021) 9305 (<https://doi.org/10.3390/ijms22179305>)
57. X. Zhai, S. Shan, J. Wan, H. Tian, J. Wang, L. Xin, *Neurotox. Res.* **40**(5) (2022) 1369-1379 (<https://doi.org/10.1007/s12640-022-00570-y>)
58. F. D. Koca, G. Ünal, M. G. Halici, *J. Nano Res.* **59** (2019) 15-24 (<https://doi.org/10.4028/www.scientific.net/JNanoR.59.15>)
59. M. I. Alkhalaf, R. H. Hussein, A. Hamza, *Saudi J. Biol. Sci.* **27** (2020) 2410-2419 (<https://doi.org/10.1016/j.sjbs.2020.05.005>).